Iranica Journal of Energy & Environment 4 (4): 361-375, 2013
ISSN 2079-2115
IJEE an Official Peer Reviewed Journal of Babol Noshirvani University of Technology
DOI: 10.5829/idosi.ijee.2013.04.04.08

BUT

Performance of Activated Carbon from Cassava Peels for the Treatment of Effluent Wastewate

[1]I.R. Ilaboya, [2]E.O. Oti, [3]G.O. Ekoh and [4]L.O. Umukoro

[1,2]Department of Civil Engineering, Faculty of Engineering,
University of Benin, PMB 1154, Benin City, Nigeria
[3]Akanu Ibiam Federal Polytechnic Unwana Afikpo, Nigeria
[4]Igbinedion University, Okada, Edo State, Nigeria

(Received: May 7, 2013; Accepted in Revised Form: Dec. 10, 2013)

Abstract: Activated carbon from cassava peels was prepared and characterized for various physiochemical properties such as moisture content, volatile matter and surface area. The effects of various parameters such as adsorbent dose, contact time, adsorption temperature and pH were studied to optimize the conditions for maximum adsorption. The mechanism of the rate of adsorption was studied using the pseudo – first order lagergren equation, Svante Arrhenius equation and the Gibbs free energy equation was used for the determination of adsorption thermodynamics. The adsorption isotherms were described by means of Freundlich and Langmuir isotherm equations and also Temkin isotherm equation which considered the effects of indirect adsorbent/ adsorbate interactions on adsorption process. The fitness of the data was measured using the value of the coefficient of correlation (R^2). The thermodynamic constant (K_{ad}), standard free energy ($\Delta G°$), enthalpy ($\Delta H°$) and entropy ($\Delta S°$) were calculated for predicting the nature of adsorption. Results obtained show the effectiveness of activated carbon from cassava peels as suitable adsorbent for the treatment of effluent wastewater

Key words: Adsorption · Wastewater · Activated carbons · Cassava peels · Commercial activated carbon

INTRODUCTION

Extensive industrial activities has caused many water bodies receiving loads of heavy metals that exceed the maximum permissible limit of wastewater discharged to protect the environment, human and animal [1]. Environmental hazards caused by the discharged of untreated wastewater into water bodies has become a major issue of great concern. Prolong inhalation of lead particles, coupled with the discharge of unused lead acid batteries into water bodies for example could result in a further increase in the risk of liver cancer [2].

Lead and other heavy metals possess the tendency to bio-accumulate in human bio systems. These heavy metals are not biodegradable and their presence in streams and lakes leads to bioaccumulation in living organism, causing health problems in animals, plants and human beings [3, 4].

A number of treatment methods for the removal of heavy metal ions from waste water have being reported in various literatures to include among others; electrodialysis, reverse osmosis, electrolytic precipitation, ion exchange etc [5].

Most of these methods suffer from draw back such as high capital, operational cost, time consumption, equipment complexity and the disposal of the residual metal sludge [6]. Adsorption offers the best solution since the process is cheap, fast and fewer complexes coupled with the fact that sophisticated equipments are not required to conduct the experiments [7].

Corresponding Author: Ilaboya Idowu Rudolph, Department of Civil Engineering, Faculty of Engineering, University of Benin, PMB 1154, Benin City, Nigeria. Mob: +2348038027260, E-mail: id_rudolph@yahoo.com

Many reports have appeared on the development of low cost and readily available adsorbents [8]. Activated carbons with their large surface area, micro porous character and the chemical nature of their surface have endear them as suitable materials (adsorbents) for the treatment of industrial and domestic wastewater especially in the removal of heavy metals from wastewater [9].

In this particular studies, activated carbon prepared from cassava peels and a commercially available activated carbon had been used to remove lead from wastewater. Adsorption parameters such as pH, contact time, temperature and dose were studied. In addition to the determination of the rate constant, equilibrium constant and other thermodynamic parameters such as the adsorption enthalpy, entropy and free energy content are defined.

MATERIALS AND METHODS

Wastewater Collection/Characterization: The wastewater was collected from an abandoned, stagnant non-flowing local pond subjected to serious abuse from the activities of men and was subjected to laboratory analysis and evaluation after conditioning at 32°C ±1, for three days in other to ascertain the physical and chemical composition.

Turbidity Measurement: The turbidity of the effluent wastewater which defines the amount of colloidal and residual suspended matter present in the wastewater was determined using the Jenway 6035 Turbidimeter.

Hydrogen Ion Concentration (pH): The hydrogen ion concentration (pH) of the waste water was determined using a standard laboratory digital micro processor pH meter; Hanna pH 210 model.

Dissolved Oxygen Content (DO): The dissolved oxygen content (DO) of the wastewater was measured using a standard laboratory sized digital dissolved oxygen analyser model: DO – 5509.

Conductivity Measurement: The conductivity of the wastewater was determined using a digital water/sand quality test kit, model AVI-660.

Heavy Metal Determination: The concentration of heavy metal (lead) present in the waste water was determined using AAS). (SOLAAR 969 UNICAM SERIES, using air acetylene flame).

Preparation/Characterization of Activated Carbon:

Commercial Activated Carbon: Commercially available activated carbon (CAC) was obtained from Qualikems Laboratory Reagents with all the standard characteristics correctly documented.

Activated Carbon from Cassava Peels: Peelings of cassava were collected from local waste deposit. The peelings were transported to the laboratory for immediate use. The peels were thoroughly washed with distilled water, dried and pulverized. Carbonization was done using the method recommended by Ekpete and Horsfall [10] with slight modification as follows. A predetermined weight of the pulverized sample was placed in a muffle furnace which allows limited supply of air at a temperature of 350°C for 30 - 60 minutes. The carbonized samples were then activated using the method recommended by Mansfield [11] with slight modification as follows: 25g of the charred sample was soaked in 250 ml of 5.5M $ZnCl_2$ solution. The mixture was thoroughly mixed until it formed a paste. The paste was then transferred to an evaporating dish which was placed in a furnace and heated at 200°C for thirty minutes. This was allowed to cool and washed with distilled water to remove the residual salt, oven dried at 105°C for one hour, grind using mortar and pestle and sifted with 106μm Standard Tyler Sieve. The activated carbon was then characterized for its particle sizes, moisture content, ash content, volatile matter, Methylene blue number, iodine number etc.

Performance of Activated Carbon

Determination of pH: (ASTM D3838-80) was employed in the determination of pH. 1.0g of activated carbon was weighed and transferred into a beaker. 100ml of distilled water was measured and added and stirred for one hour. The samples were allowed to stabilize before the pH was measured using a digital pH meter [10].

Iodine Number Determination: In determining the iodine number, 10 ml of 5% by weight HCl was added to 1g of activated carbon and was allowed to boil for 30 seconds. After the solution was cooled to room temperature, 100ml of 0.1N iodine solution was added. The content was shaken vigorously and filtered. 25 ml of the filtrate was titrated against 0.1N sodium thiosulphate using starch as indicator. The iodine number was defined as the quantity of iodine adsorbed in (mg/g carbon) as residual iodine concentration (ASTM, D4607-94).

Methylene Blue Number: The Methylene blue number is defined as the maximum amount of dye adsorbed on 1.0g of adsorbent. In this method, 1g of activated carbon was placed in contact with 10.0ml of 25mg/l Methylene blue solution for 24 hours at room temperature followed by intermittent shaking. The solution was thereafter filtered using Whatman number one filter paper and an aliquot solution was taken for analysis. The remaining concentration of Methylene blue was analyzed using an Atomic Adsorption Spectrophotometer. The amount of Methylene blue adsorbed was calculated using the mass balance equation 3.5 [12].

Moisture Content Determination (MC %): Thermal drying method was used in the determination of moisture content of the samples. 1.0g of the dried activated carbons was weighed and placed in washed, dried and weighed crucible. The crucibles were placed in an oven and dried at 105°C to constant weight for 1 hour. The percentage moisture content (MC %) was computed as follows [13].

$$(\text{MC }\%) = \frac{\text{Loss in weight on drying}}{\text{Initial weight of sample}} \times 100 \quad (1)$$

Ash Content Determination (AC %): The standard test method for ash/volatile matter content-ASTM D2866-94 was used.

- 1.0g activated carbon was taken, dried in an oven at a temperature of 105°C for 1h.
- The final weight after drying was measured and recorded as (Xg = Oven dry weight).
- Thereafter the dried activated carbon was placed in a cold muffle furnace and the temperature was allowed to rise until it reaches 500°C.
- It was removed and allowed to cool in a desiccator to room temperature and reweighed again and its weight was again recorded as (Yg = Ash weight).

The percentage ash content was then determined

$$(\text{AC }\%) \frac{\text{Ash Weight (g)}}{\text{Oven Dry Weight (g)}} \times 100 \quad (2)$$

Volatile Matter Determination (VM %): The standard test method for ash/volatile matter content-ASTM D2866-94 was used.

- 1.0g activated carbon was taken, dried in an oven at a temperature of 105°C for 1h.
- The final weight after drying was measured and recorded as (Xg = Oven dry weight).
- Thereafter the dried activated carbon was placed in a cold muffle furnace and the temperature was allowed to rise until it reaches 500°C.
- It was removed and allowed to cool in a desiccator to room temperature and reweighed again and its weight was again recorded as (Yg = Ash weight).

The percentage volatile matter was then determined as follows:

$$(\text{VM }\%) \frac{(\text{Xg-Yg})}{\text{Oven dry weight}} \times 100 \quad (3)$$

Particle Size Determination: A standard set up for particle size determination using variable sieve sizes arranged in descending order of mesh sizes was used. The idea was to ensure that a uniform particle size was used for the different adsorbent including the commercially available adsorbent [14].

Surface Area, Micropore Volume and Total Pore Volume Estimation Using the Iodine and Methylene Blue Number: The surface areas of activated carbon are usually measured using the Brunauer Emmentt and Teller (BET) method which employs the nitrogen adsorption at different pressures at the temperature of liquid nitrogen (77°K); the total pore volume is estimated from the amount of nitrogen adsorbed at the highest relative pressure and the micropore volume is calculated from the nitrogen adsorption isotherm using the Dubinin – Radushkevich equation. Inspite of these method being more used and employed as a reference in the surface area and pore volume determination of porous material, they are also time consuming and require the use of highly sophisticated equipments such as porosimeter, scan electron microscope (SEM) and Fourier transform infrared spectrophotometer (FT_IR).

Additional information regarding the structure of activated carbon can be obtained using the adsorption characteristics of the adsorbent such as the iodine and the Methylene blue number. Adsorption experiments of these molecules are very easy and do not require the use of highly sophisticated equipment. Information regarding the iodine number and Methylene blue number are important indicators on the adsorption capacity of the adsorbent materials hence was employed in computing the surface area, pore volume and micro pore volume. The iodine and Methylene blue numbers were determined

using standard methods as described in 2.3.2 and 2.3.3 respectively. Data obtained were fitted into (SCAC-Structural Characterization of Activated Carbon) software to compute the surface area, micropore and total pore volume respectively [12].

Investigation of Adsorption Parameters

Effects of Temperature: In order to investigate the effect of temperature on the overall adsorption process, 12g activated carbon prepared from each material was contacted with 100ml of the wastewater in a 250ml beaker. The mixture was placed in a constant temperature water bath maintained at a temperature of 15°C for an equilibrium adsorption time of 2 hours (120 minutes) under a constant stirring speed of 50rpm. The mixture was then filtered using a 150mm diameter whatman filter paper and an aliquot solution was the taking for analysis using AAS (Atomic Adsorption Spectrophotometer) to determine the equilibrium concentration of the metal ion remaining. The same process was repeated with the bath maintained at temperature of 20, 30 and 45°C respectively.

Effect of pH: In order to investigate the effect of pH on the overall adsorption process, the wastewater was maintained at pH of 2, 4, 6, 8, 10 and 12 by adding a 1 molar concentration of calcium hydroxide and hydrochloric acid and then monitoring the pH using a digital pH meter fitted with calomel electrode. As soon as the desired pH was achieved, 12g activated carbon was added under a constant stirring speed of 50rpm for an equilibrium adsorption time of 2 hours. The experimental temperature was maintained at 30°C and the equilibrium concentration of the metal ion remaining was determined using AAS (Atomic Adsorption Spectrophotometer).

Effect of Adsorbent Dosage: One of the parameters that strongly affect the sorption phenomenon is the dose of the adsorbents. This may be due to the increase in availability of surface active sites resulting from the increased dose of the adsorbent [15]. In this research project, adsorbent dose of 0, 2, 4, 6, 8, 10 and 12g were selected at adsorption temperature of 30°C to determine the effects of adsorbent dosage on the overall adsorption process.

Effect of Contact Time: The kinetic studies were performed to determine the adsorption rates of the adsorbent and the minimum contact time for adsorption. In this experiment, 12g of the adsorbent was contacted with 100ml of solution in each sample bottle at adsorption temperature of 34°C. The content was stirred using a magnetic stirrer for different increment of time ranging from 0, 20, 40, 60, 80, 100 and 120 minutes. Samples were collected at the different time intervals, filtered through Whatman No. 1 filter paper and an aliquot solution was taken for analysis to determine the equilibrium concentration and the overall effects of contact time on the adsorption process.

Adsorption Efficiency: The impact of adsorption process was studied by monitoring the overall effects of adsorption on the following indices:

- Impact on Conductivity
- Impact on Dissolved Oxygen
- Amount of metal ion removed:

Conductivity/dissolved oxygen level were measured before and after adsorption and the amount of heavy metal ions removed during the series of batch investigation was determined using the mass balance equation as proposed by [16]:

$$q = \frac{v}{m}[C_0 - C_e] \tag{4}$$

where: q, defines the metal uptake [mg/g]; C_0 and C_e: are the initial and equilibrium metal ion concentrations in the wastewater [mg/l] respectively; V: is the waste water sample volume (ml) and M: is the mass of adsorbent used [g].

The efficiency of metal ion removal (%) was calculated using the following mass balance equation stated as follows [17]:

$$\left(\frac{C_0 - C_e}{C_0} \times 100\right) \tag{5}$$

where: C_0 and C_e are the metal ion concentrations (mg/l) in the wastewater sample before and after treatment respectively.

Adsorption Isotherm Studies: The adsorption isotherm indicates how the adsorbent molecules distribute themselves between the liquid phase and the solid phase when the adsorption process reaches an equilibrium state. It is the equilibrium relationship between the amount of adsorbate removed and the amount remaining [18]. In this study, the experimental isotherm data set obtained were fitted using adsorption models including Langmuir,

Freundlich and Temkin isotherms. The applicability of the isotherm equations was compared by judging the correlation coefficient, R^2 [19].

Freundlich Isotherm Model: The monolayer Freundlich isotherm is an indication of the extent of heterogeneity of the adsorbent surface. The general form of the isotherm is given as follows:

$$q = K_f C_e^{\frac{1}{n}} \quad (6)$$

where:

q = Amount adsorbed (g)
K = Freundlich capacity constant
C_e = Equilibrium concentration (ppm)
1/n = Freundlich intensity parameter

A linear form of this expression is given as [log (q) = log (K_f) +1/n log (C_e)] and values of K and n were calculated from the intercept and slope of the plot of [log (q) against log C_e] [20].

Langmuir Isotherm Model: The Langmuir adsorption isotherm is based on the theoretical principle that only a single adsorption layer exists on an adsorbent and it represents the equilibrium distribution of metal ions between the solid and liquid phases. The basic assumption of the Langmuir adsorption process is the formation of a monolayer of adsorbate on the outer surface of the adsorbent and after that no further adsorption takes place [20]. The Langmuir Isotherm is described by the following equation:

$$q = \frac{abC_e}{bC_e + 1} \quad (7)$$

This equation can be rearranged to yield the following linear expression:

$$\frac{Ce}{q} = \left(\frac{Ce}{a}\right) + \frac{1}{ab} \quad (8)$$

where: q is the amount of metal adsorbed per unit mass of adsorbent (g), [a] and [b] are the Langmuir constants and are indicative of adsorption capacity (mg/g) and energy of adsorption (l/mg) respectively and Ce is the equilibrium concentration of adsorbate in waste water sample after adsorption (mg/l). The Langmuir constants [a] and [b], were obtained from the intercept and slope of the plot of (Ce/q) against (Ce).

Temkin Isotherm Model: Temkin considered the effects of indirect adsorbent/adsorbate interactions on adsorption isotherms. The heat of adsorption of all the molecules in the layer would decrease linearly with coverage due to adsorbent/ adsorbate interactions. The Temkin isotherm has been used in the following equation:

$$q = a + b \ln C_e \quad (9)$$

where: q is the amount adsorbed, C_e is the equilibrium concentration, a and b, are the Temkin constants. Therefore a plot of q vs. ln Ce enables one to determine the constants a and b [19].

Thermodynamic Parameters: The following thermodynamics parameters were studied:

Activation Energy Determination: The activation energy of adsorption helps to determine the minimum amount of energy that the adsorbate molecules need to break through the tiny inter phase and react with the active site of the adsorbent so as to cause separation from the bulk solution (film diffusion). Activation energy of the adsorption process was determined using Svant Arrhenius equation stated as follows:

$$K = Ae^{\frac{-E}{RT}} \quad (10)$$

where K is the rate constant of the adsorption process, A is the frequency factor, R is the molar gas constant, T is the thermodynamic absolute temperature and E is the value of the activation energy of the adsorption process (21). The linearized form of the equation is given as:

$$\ln K = \ln A - \frac{E}{RT} \quad (11)$$

A linear plot of ($\ln K_{ad}$) against 1/T gives an intercept that is equal to lnA and a slope that is equal to –E/R from where the activation energy of the adsorption process can be determined [19].

Adsorption Rate Constant: The rate constant of adsorption (K_{ad}) measures the time domain for the adsorption process; it is the time dependent study of adsorption process. The first order rate constant for the adsorption of metal ion on the granular activated carbon was studied using the Lagergren equation [22].

$$\log[q_e - q] = \log q_e - \frac{K_{ad}t}{2.303} \quad (12)$$

where: q_e and q are the amount of a specific metal ion adsorbed at equilibrium and at time t respectively, K_{ad} = the rate constant for the adsorption of a specific metal ion. The linear plot of log (q_e – q) versus time (t) shows the appropriateness of the above equation and the first order nature of the adsorption process [22].

Adsorption Equilibrium Constant: The adsorption equilibrium constant (K_c) measures the maximum rate of adsorption at time t. For most standard adsorption process, t is usually taken as 1h. This is subject to change depending on the nature of the experimental set up [23]. The adsorption of metal ion on activated carbon can be expressed as:

$$A + M \underset{K_2}{\overset{K_1}{\longleftrightarrow}} [A] + [M] \quad (13)$$

where: A, is the activated carbon; M is the metal ion; K_1 and K_2 are the rate constant for the forward (adsorption) and the backward (desorption) Processes respectively. The equilibrium constant K_C can be calculated as; [23].

$$K_C = K_1 / K_2 = C_L / C_S \quad (14)$$

where: C_L and C_S are the equilibrium concentrations of metal ion on activated carbon and in solutions respectively. Mathematically these concentrations can be expressed as;

$$C_L = C_i (F) \text{ and } C_S = C_i (1-F) \quad (15)$$

where: C_i is the initial concentration of metal ions and F is the fractional amount of adsorption at equilibrium. Substituting C_L and C_S into the above equation gives;

$$K_C = (F) / (1-F) \quad (16)$$

where;

$$F = \frac{C_{ao} - C_a}{C_{ao}} \quad (17)$$

C_{ao} and C_a represent the initial and equilibrium concentration of metal ion.

Enthalpy, Entropy and Free Energy Content: Thermodynamic constants such as the enthalpy (ΔH) help to classify adsorption as either an exothermic or endothermic process. The entropy value (ΔS) and the free energy constant (ΔG) allow for studies on the degree of randomness at the solid – solution interface during the fixation of metal ion on the active site of the adsorbent and the spontaneity of the process (i.e., whether adsorption is spontaneous or non-spontaneous). The thermodynamic quantities; ΔG, ΔH and ΔS of metal ion adsorption on the activated carbon were calculated using the following relations [19].

$$\text{Ln}K_C = [-\Delta H / RT] \quad (18)$$
$$\Delta G = [-RT \ \text{ln}K_C] \quad (19)$$
$$\Delta S = [(\Delta H - \Delta G) / T] \quad (20)$$

where T is thermodynamic temperature, R is the molar gas constant (8.314 J/gmol.K)). The value of ΔH was computed from the slope of the linear variation of $\text{ln}K_C$ and the inverse of adsorption temperature.

RESULTS AND DISCUSSION

Table 1 shows the physico-chemical properties of the wastewater used. The results reveal a high level of pollution especially in terms of heavy metal ion concentration when compared to World Health Organisation standard.

Table 2 shows the properties of activated carbon use in the studies.

CAC, ACP: Commercial Activated Carbon and Activated Cassava Peels respectively.

The effect of pH on the adsorption of lead and copper is shown in Figures 1 and 2 below:

The removal of metal ions from wastewater sample by adsorption is related to the pH of the samples, as the later affects the surface charge of adsorbents, the degree of ionization and the species of adsorbate. The amount of lead and copper ion adsorbed increases with increasing pH and reach a maximum at pH of 8 and then begins to decrease. An increase in metal uptake as pH increases can be explained on the basis of a decrease in competition between hydroxonium ions and metal species for the surface sites and also by decrease in positive surface charge on the adsorbent, which result in a lower electrostatic repulsive force between the surface and the metal ions and hence uptake of metal ions increases [24, 25, 26, 27].

Figures 3 and 4 show the effect of adsorbent dosage on metal uptake.

Table 1: Effluent Wastewater Component

S/no	Parameters	Result
1	Turbidity	18.7(NTU)
2	pH	2.3
3	Conductivity	256 (µs/m)
4	Dissolved Oxygen	0.3(mg/l)
5	Lead	5.25(mg/l)
6	Copper	4.03(mg/l)
7	Temperature	32(°C)

Table 2: Properties of Activated Carbon

S/No	Parameter	CAC	ACP
1	Ash Content (%)	5.1	6.7
2	Moisture Content (%)	4.33	8.7
3	Total Pore Volume (ml/g)	0.67	0.24±0.03
4	Iodine Number	585	543
5	Surface Area (m^2/g)	625	460±50
6	Volatile Matter	1.7	4.6
7	Mean Particle Size (mm)	0.106	0.106
8	Apparent Density (g/mL)	0.56	-
9	Fixed Carbon	66.75	-
10	pH	6.5	6.8
11	Methylene Blue Number	-	27
12	Micropore volume (ml/g)	-	0.14±0.02

It could be deduce from Figures 3 and 4 that an increase in the dose of CAC and ACP resulted in an increase in efficiency of metal (Pb^{2+} and Cu^{2+}) uptake reaching up to about 80% to 84% for CAC and 74% to 77% for ACP. Higher dosage of adsorbent will increase the adsorption due to more surfaces and functional group of the adsorbents on which the metal could interact with. More also, an improvement in the dissolved oxygen value and a slight reduction in the electrical conductivity of the effluent wastewater was seen with increasing dose of the adsorbents as shown in Figure 5 and 6, respectively.

Adsorption is not aimed at removing TDS from wastewater hence the inability of the process to address the conductivity problem of the effluent wastewater.

The effect of contact time on metal uptake was also studied and it was observed that, the percent removal of heavy metal ion and the amount of heavy metal ion adsorbed increases with increase in contact time as shown in Figures 7 and 8, respectively.

Figures 7 and 8 show the graphical variation between the percentage removal of heavy metal and contact time using 12g/l of activated carbon from CAC and ACP, at pH 8, agitation of 50rpm for fixed initial metal ion concentration of 5.25mg/l Pb^{2+} and 4.03mg/l Cu^{2+}.

Adsorption data obtained were analyzed in the light of Freundlich, Langmuir and Temkin isotherm models. Results obtained are presented in Figures 9, 10, 11, 12, 13 and 14, respectively.

Table 3: Isotherm Constants for Pb^{2+} adsorption

Freundlich Isotherm Constants			
	Pb^{2+} Adsorption		
Adsorbent	k_f	N	R^2
CAC	1.00	0.63	0.937
ACP	1.20	0.63	0.966
Langmuir Isotherm Constants			
	Pb^{2+} Adsorption		
Adsorbent	a (mg/g)	b (l/mg)	R^2	R_L
CAC	9.25	0.14	0.972	0.58
ACP	5.00	0.20	0.972	0.49
Temkin Isotherm Constants			
	Pb^{2+} Adsorption		
Adsorbent	a (mg/g)	b (l/mg)	R^2
CAC	37	23.54	0.978
ACP	38	31.33	0.981

Table 4: Isotherm Constants for Cu^{2+} adsorption

Freundlich Isotherm Constants			
	Cu^{2+} Adsorption		
Adsorbent	k_f	n	R^2
CAC	0.75	0.71	0.929
ACP	1.50	0.71	0.936
Langmuir Isotherm Constants			
	Cu^{2+} Adsorption		
Adsorbent	a (mg/g)	b (l/mg)	R^2 Adsorbent	R_L
CAC	8.33	0.24	0.977	0.51
ACP	7.00	0.22	0.954	0.53
Temkin Isotherm Constants			
	Cu^{2+} Adsorption		
Adsorbent	a (mg/g)	b (l/mg)	R^2
CAC	25	12.92	0.954
ACP	27	17.15	0.982

Tables 3 and 4 show the isotherm constants for Pb^{2+} and Cu^{2+} ion adsorption unto CAC and ACP, respectively.

The high values of the correlation coefficient (R^2) obtained indicates the fitness of the adsorption data to the model used hence the suitability of CAC and ACP in the removal of Pb^{2+} and Cu^{2+}.

The separation factor R_L indicates the isotherm shape and whether the adsorption process is favourable or not [28, 29]. Since R_L values falls between 0 and 1, the adsorption of Pb^{2+} and Cu^{2+} ion unto CAC and ACP is therefore classified as favourable.

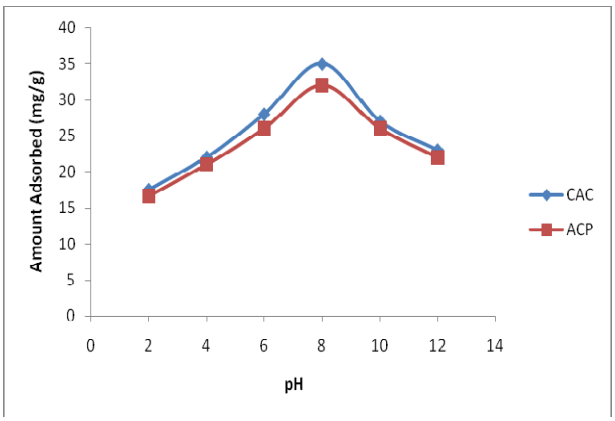

Figure 1:Effect of pH on Pb^{2+} uptake

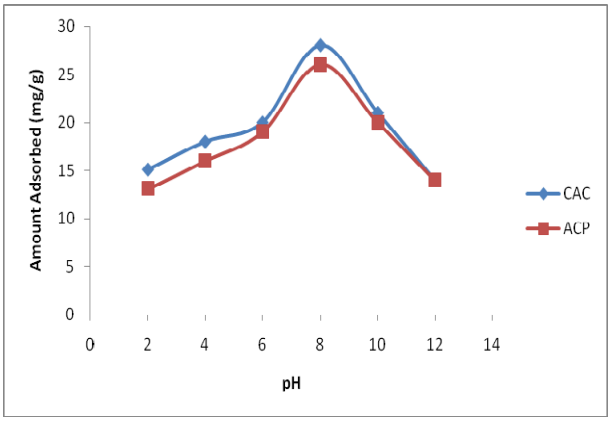

Figure 2:Effect of pH on Cu^{2+} uptake

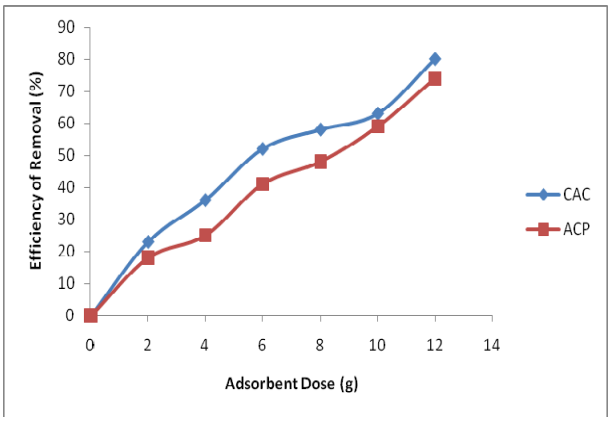

Figure 3: Effect of adsorbent dosage to the adsorption efficiency of Pb^{2+}

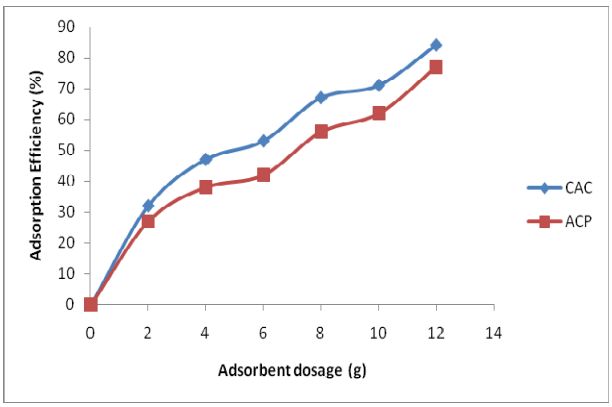

Figure 4: Effect of adsorbent dosage to the adsorption efficiency of Cu^{2+}

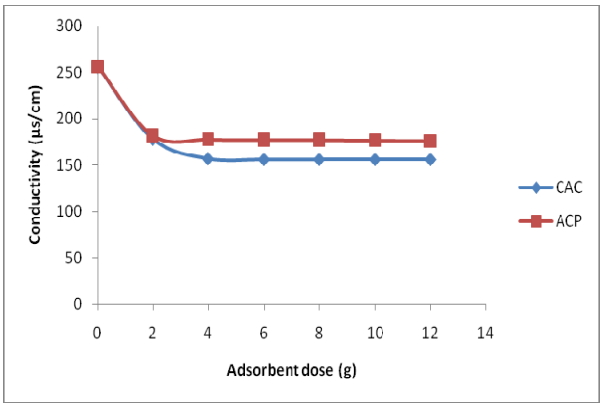

Figure 5: Effect of adsorbent dosage on conductivity of effluent wastewater

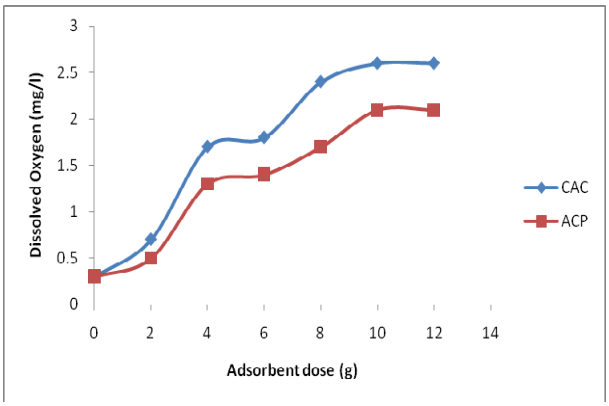

Figure 6: Effect of adsorbent dosage on dissolved oxygen of effluent wastewater

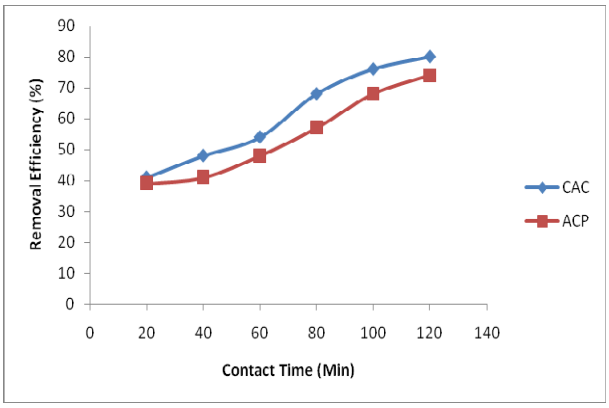

Figure 7: Effect of contact time to the adsorption efficiency of Pb^{2+}

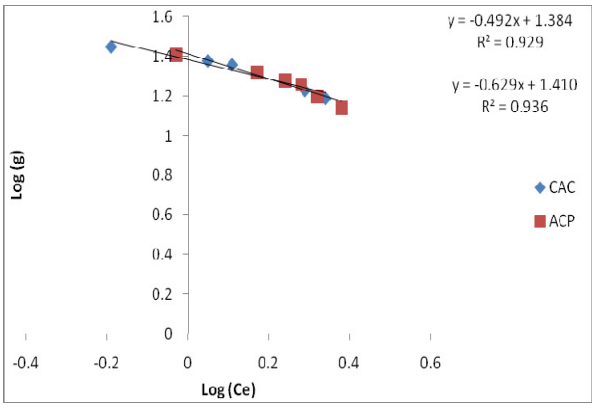

Figure 10: Freundlich Isotherm model for Cu^{2+} adsorption unto CAC and ACP

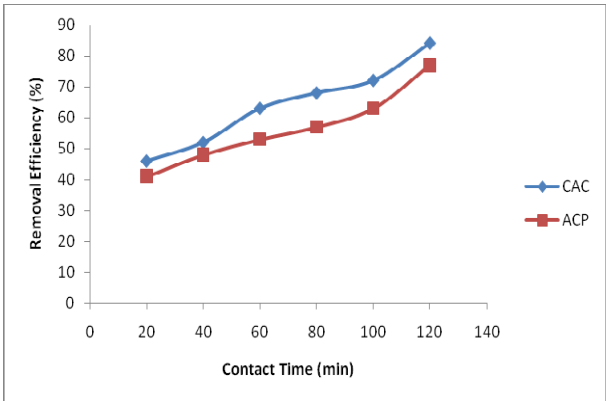

Figure 8: Effect of contact time to the adsorption efficiency of Cu^{2+}

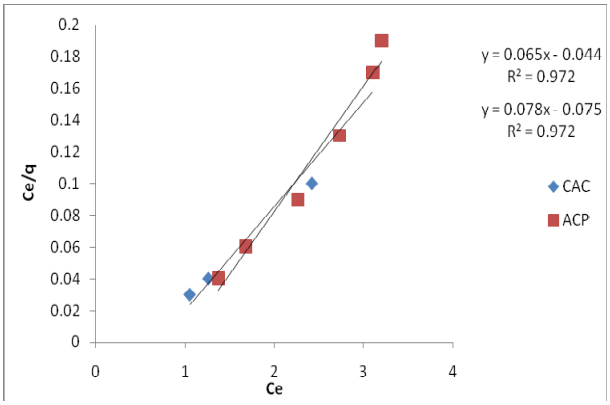

Figure 11: Langmuir Isotherm model for Pb^{2+} adsorption unto CAC and ACP

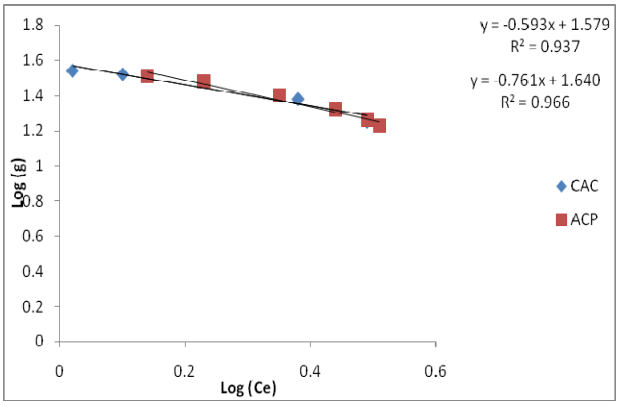

Figure 9: Freundlich Isotherm model for Pb^{2+} adsorption unto CAC and ACP

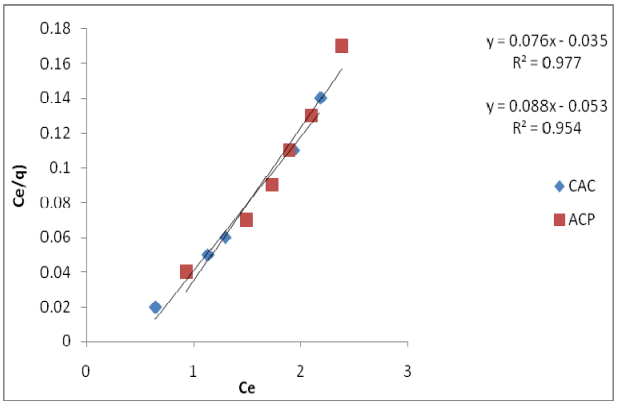

Figure 12: Langmuir Isotherm model for Cu^{2+} adsorption unto CAC and ACP

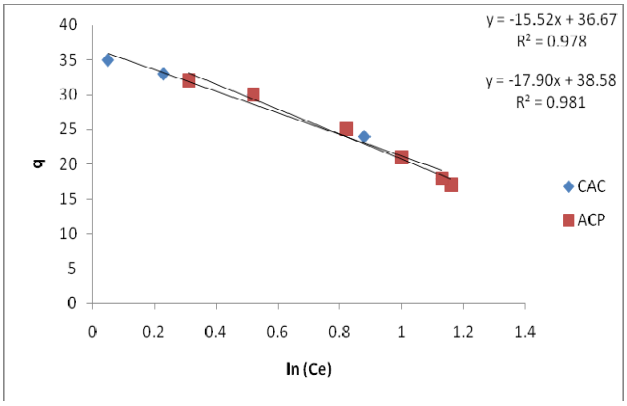

Figure 13: Temkin Isotherm model for Pb^{2+} adsorption unto CAC and ACP

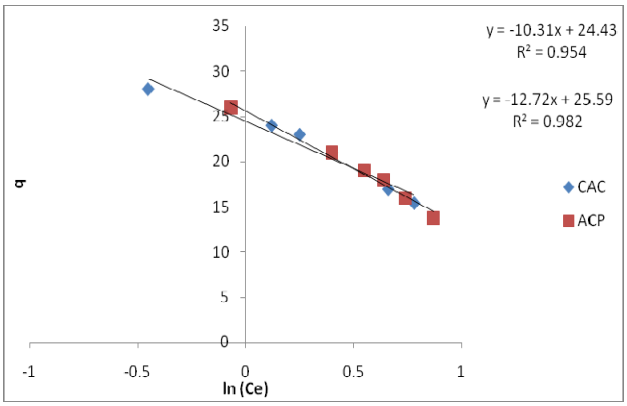

Figure 14: Temkin Isotherm model for Cu^{2+} adsorption unto CAC and ACP

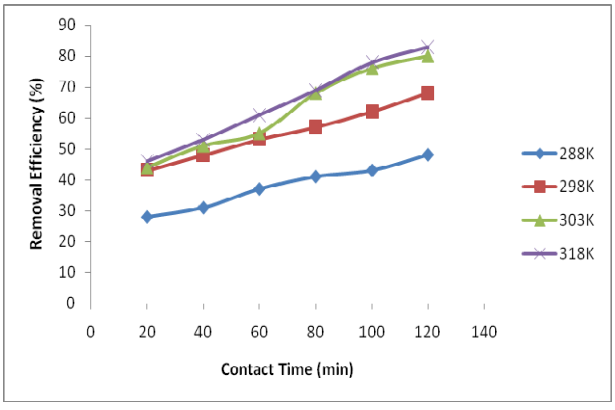

Figure 15: Effect of temperature on Pb^{2+}adsorption unto CAC

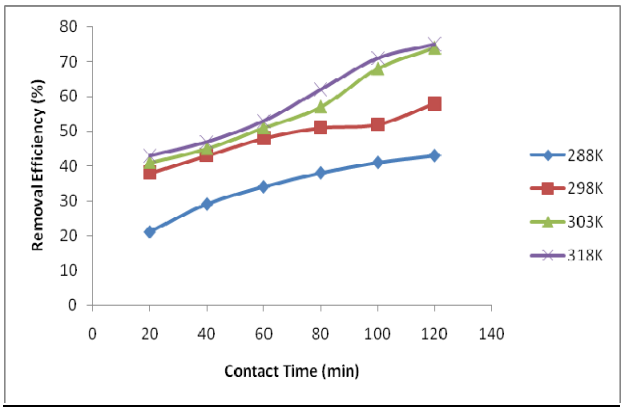

Figure 16: Effect of temperature on Pb^{2+}adsorption unto ACP

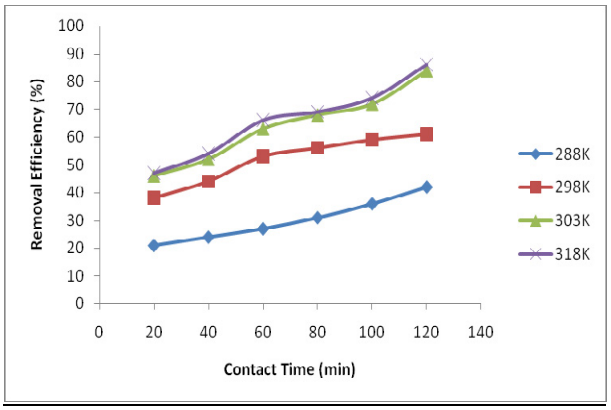

Figure 17: Effect of temperature on Cu^{2+}adsorption unto CAC

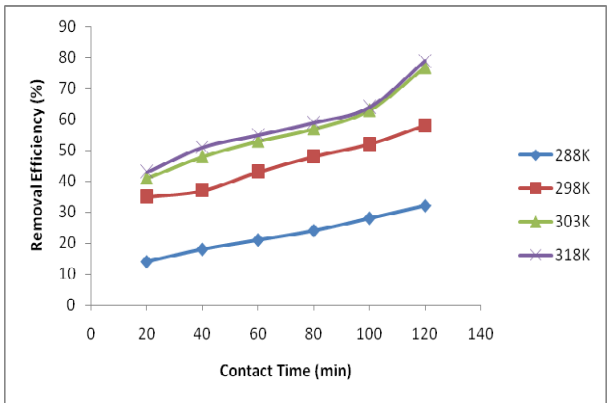

Figure 18: Effect of temperature on Cu^{2+}adsorption unto ACP

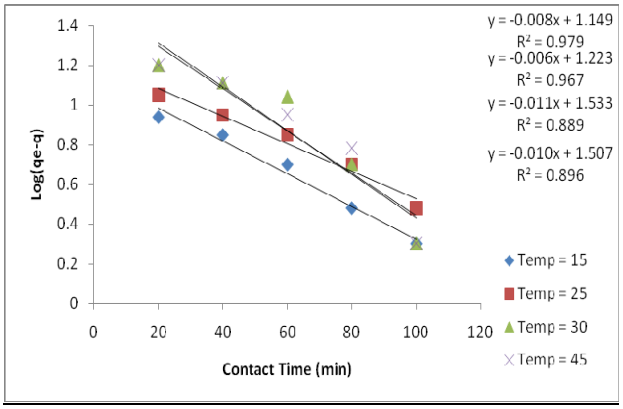

Figure 19: Plots of log (qe-q) versus time for Pb^{2+} ion adsorption onto CAC

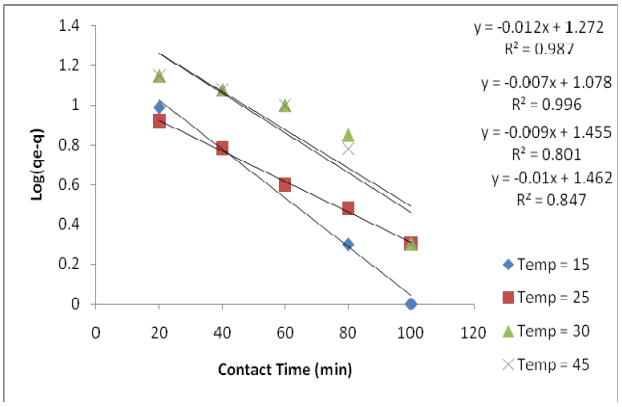

Figure 20: Plots of log (qe-q) versus time for Pb^{2+} ion adsorption onto ACP

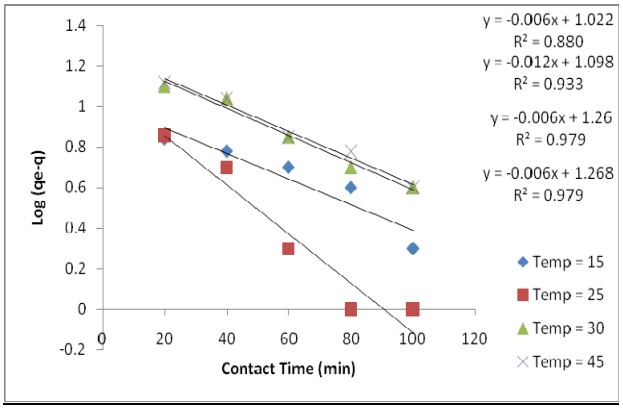

Figure 21: Plots of log (qe-q) versus time for Cu^{2+} ion adsorption onto CAC

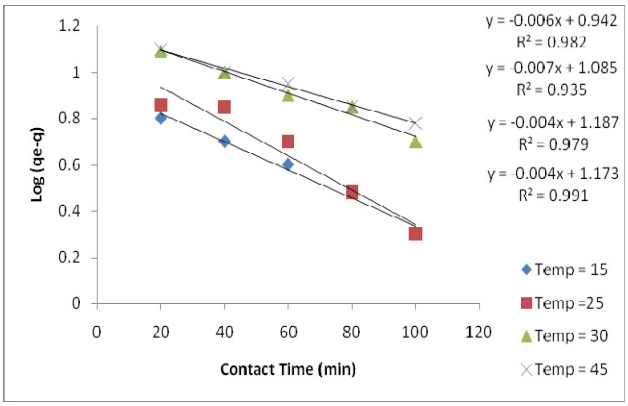

Figure 22: Plots of log (qe-q) versus time for Cu^{2+} ion adsorption onto ACP

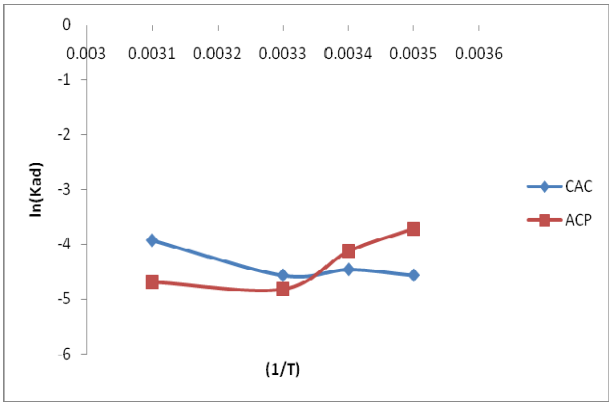

Figure 23: Activation energy computation for Pb^{2+} ion adsorption

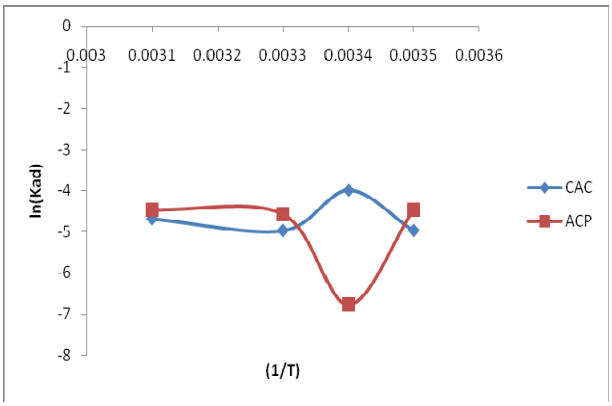

Figure 24: Activation energy computation for Cu^{2+} ion adsorption

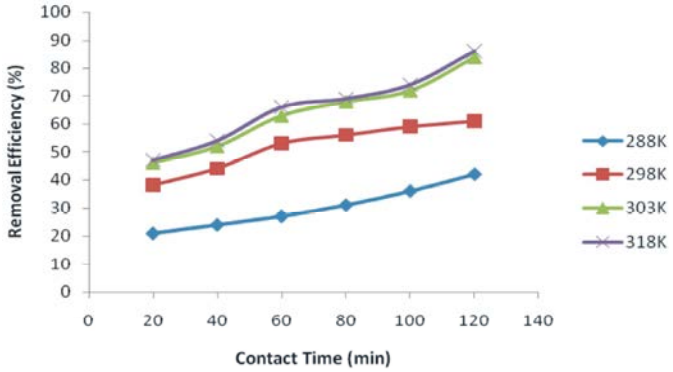

Fig. 17: Effect of temperature on Cu^{2+}adsorption unto CAC

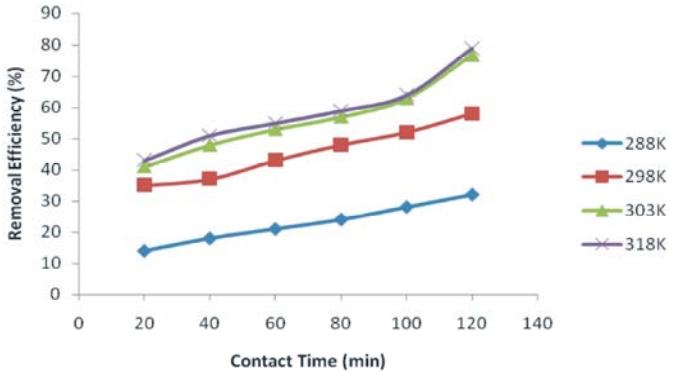

Fig. 18: Effect of temperature on Cu^{2+}adsorption unto ACP

The adsorption of metal ions was found to increase with an increase in temperature. The increase in adsorption capacity of activated carbon with temperature indicates an endothermic process. The graphical variation between the efficiency of removal (%) and contact time at varying adsorption temperature are shown in Figures 15, 16, 17 and 18, respectively.

Temperature variation influences the amount of lead and copper ions adsorption, which increases with the rise in adsorption temperature. This is because at higher temperature, the diffusion of metal ions through the activated carbon pores is faster and can proceed to a larger extent [23, 30].

The rate constant of the adsorption process was determined using Lagergren equation of the form;

$$\text{Log}\,[q_e - q] = \log\,[q_e] - \frac{K_{ad}t}{2.303} \quad (21)$$

where; q_e and q are the amount adsorbed at equilibrium and at time (t), respectively. Mathematically:

$$\log[q_e - q] = \log q_e - \frac{K_{ad}t}{2.303} \quad (22)$$

where

$-\frac{K_{ad}}{2.303} =$ slope and

$-2.303\,[slope] = K_{ad}$

The linear plots of Log $[q_e - q]$ versus time on shows the appropriateness of the above equation and subsequently the first order nature of the adsorption process [30, 31]:

The value of the rate constant K_{ad} were calculated from the slope of Figures 19, 20, 21 and 22, respectively. These values were then fitted into the Svant Arrhenius equation to determine the activation energy of the adsorption process:

Figures 23 and 24 show the linear plot of $\ln K_{ad}$ versus (1/T) with slope equals -(E/R) and intercept as lnA. Where E; is the Activation Energy and R; is the molar gas constant.

Values of the activation energy obtained for Pb^{2+} and Cu^{2+} ion adsorption onto CAC and ACP are 8.765Kj/mol and 11.965Kj/mol for CAC, 5.554Kj/mol and 4.382Kj/mol for ACP. The results show a positive value of activation energy for the adsorption of lead ion and copper ion onto CAC and ACP.

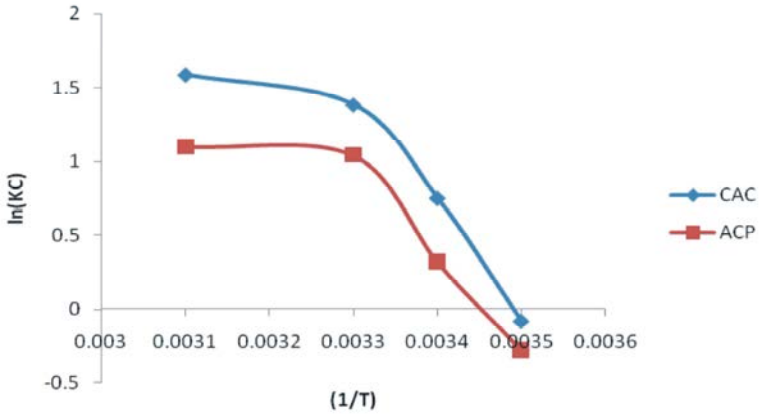

Fig. 27: lnKc versus reciprocal of temperature (1/T) for Pb^{2+} ion adsorption

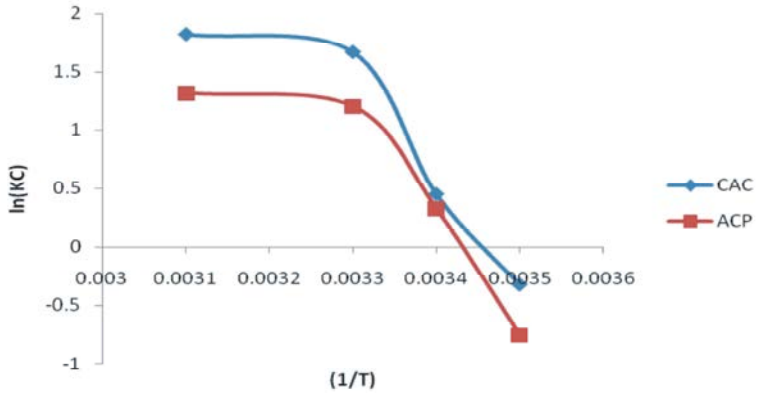

Fig. 28: lnKc versus reciprocal of temperature (1/T) for Cu^{2+} ion adsorption

The values of the equilibrium constant (K_C) for the adsorption Pb^{2+} and Cu^{2+} ions onto CAC and ACP were calculated at different temperatures for an equilibrium adsorption time of 120 minutes, results obtained are shown in Figures 25 and 26, respectively.

The result shows that (K_C) values increases with increase in adsorption temperature for lead and copper ion adsorption, thus implying a strengthening of the adsorbate-adsorbent interactions with increasing adsorption temperature.

The thermodynamic quantities such as ΔG, ΔH and ΔS for lead ion and copper ion adsorption were calculated from equations 18, 19 and 20. Values of ΔH were computed from the slope of the linear variation of ln (K_C) against the reciprocal of adsorption temperature (1/T) shown in Figures 27 and 28.

Values of the thermodynamic parameters for lead and copper ion adsorption are shown in Table 5 below:

The positive value of ΔH shows that the adsorption of lead ion and copper ion onto CAC and ACP is an endothermic process. The values of ΔG are negative at temperature of 298°K and above as expected for a spontaneous process.

Table 5: Thermodynamic parameter for Pb^{2+} ion adsorption

Enthalpy ΔH (J/mol)		
Temperature (K)	CAC	ACP
288	8438.7	2494.2
298	8438.7	2494.2
303	8438.7	2494.2
318	8438.7	2494.2
Free Energy ΔG = -RTlnKc (J/mol)		
Temperature (K)	CAC	ACP
288	191.51	670.28
298	-1868.09	-790.35
303	-3491.53	-2622.43
318	-4201.08	-2910.88
Entropy ΔS = [(ΔH - ΔG)/T] J/K.mol		
Temperature (K)	CAC	ACP
288	28.64	6.33
298	34.59	11.02
303	39.37	16.89
318	39.75	17.00

The decrease in ΔG value with increasing adsorption temperature reveals that adsorption of lead ion and copper ion onto CAC and ACP becomes better at higher temperature. The positive value of ΔS for the adsorption of lead ion and copper ion reveals the

Table 6: Thermodynamic parameter for Cu^{2+} ion adsorption

Enthalpy ΔH (J/mol)		
Temperature (K)	CAC	ACP
288	6526.49	4780.55
298	6526.49	4780.55
303	6526.49	4780.55
318	6526.49	4780.55
Free Energy ΔG = -RTlnKc (J/mol)		
Temperature (K)	CAC	ACP
288	778.00	1802.57
298	-1112.43	-805.21
303	-4199.41	-3033.05
318	-4822.39	-3487.24
Entropy ΔS = [(ΔH - ΔG)/T] J/K.mol		
Temperature (K)	CAC	ACP
288	19.96	10.34
298	25.63	18.74
303	35.40	25.79
318	35.69	26.00

increased randomness at the solid-solution interface during the fixation of the adsorbate ion (lead and copper) on the active site of the adsorbent.

CONCLUSION

Since the adsorption of lead ion and copper ion is endothermic, it follows that the adsorption process becomes spontaneous because of the positive entropy change. In addition cassava peels has been found to be suitable materials (adsorbents) for the treatment of waste water especially in the removal of heavy metals and other organisms that tend to alter the original properties of the water. It can thus be concluded that; Based on the values of the coefficient of correlation (R^2) calculated the Temkin isotherm model best fitted the experimental data on adsorptive behaviour of all metal ions on the various activated carbons, followed by the Freundlich isotherm model and then the Langmuir isotherm model.

The adsorption process followed a first order kinetics and pH has been found to be the most effective variable controlling the adsorption of metal ions onto activated carbons.

REFERENCES

1. Ahmad, A., B. Hameed and N. Aziz, 2007. Adsorption of direct dye on palm ash: Kinetic and equilibrium modeling. Journal of Hazardous Materials, 141(1): 70-76.
2. Ahmad, S., N. Khalid and M. Daud, 0000. Adsorption Studies of lead on Lateritic Minerals from Aqueous media, Separation Science and Technology, 37: 343-362.
3. Ong, S., C. Seng and P. Lim, 2007. Kinetics of adsorption of copper (II) and cadmium (II) from aqueous solution on rice husk and modified rice husk, electronic Journal of Environmental Agriculture and Food Chemistry, 6(2): 1764-1774.
4. Ceribas, H.I. and U. Yetis, 2001. Bisorption of Nickel (II) and Lead (II) by phanaerochate chrysosporium from Binary metal system-kinetics Water SA, 27(1): 15-20.
5. Ahmedna, M., M.M. Johns, S.J. Clarke, W.E. Marshall and R.M. Rao, 1997. Potential of agricultural by product based activated carbons for use in raw sugar decolourization, Journal of Agriculture and Food Science, 75: 117-124.
6. Amuda, O.S. and A.O. Ibrahim, 2006. Industrial waste water treatment using natural material as adsorbent, African Journal of Biotechnology, 5(16): 23-29.
7. ASTM, D4607-94, Standard method for the determination of Iodine Number of Activated Carbon.
8. Azab, M.S. and P.J. Peterson, 1989. The removal of Cadmium from wastewater by the use of biological sorbent. Water Science and Technology Journal, 21: 1705-1706.
9. Badmus, M., T. Audu and B. Anyata, 2007. Removal of lead ion from industrial wastewaters by activated carbon prepared from periwinkle shells (Typanotonus fuscatus). Turkish J. Eng. Env. Sci., 31(4): 251-263.
10. Ekpete, O.A. and Horsfall M. JNR, 2011. Preparation and Characterization of Activated Carbon derived from Fluted Pumpkin Stem Waste, Research Journal of Chemical Sciences, 1(3): 10-17.
11. Mansfield, G.R., 1998. Clay Investigation in Southern States, US Geological Survey Bulletin, 901: 1-22.
12. Cleiton, A., M. Nunese and C. Guerreiro, 2011. Estimation of Surface Area and pore volume of Activated Carbon by Methylene Blue and Iodine Numbers, Quim Nova, 34(3): 472-476.
13. Rengaraj, S., M. Seung- Hyeon and S. Sivabalm, 2002. Agricultural solid waste for the removal of organics: adsorption of phenol from water and wastewater by palm seed coat activated carbon, Waste Management, 22: 543-548.
14. Howard, S.P., R.R. Donald and G. Tchobanoglous, 2008. Prentice-Hall of India Private Limited, New Delhi, Environmental Engineering, pp: 56-78.

15. Saeed, A., M.W. Akhter and M. Iqbal, 2005. Removal and recovery of heavy metals from aqueous solution using papaya wood as a new biosorbent, Separation Technology, 45: 25-31.
16. Raghuvanshi, S.P., R. Singh and C.P. Kaushik, 2004. Kinetics studies of Methylene blue dye bio-adsorption on Baggase, Applied Ecology and Environmental Research, 2(2): 35-43.
17. Ilaboya, I.R., A.A. Erameh, O.O. Ighodaro and E. Atikpo, 2009. Adsorption of Lead on Activated Palm Nut Chaff (PNC); Influence of temperature on the kinetics of the adsorption process, African Journal of Science, 10(1): 2254-2263.
18. Ola, A., E.N. Ahmed, E.S. Amany and K. Azzak, 2005. Use of Rice Husk for Adsorption of Direct Dye from aqueous solution: A case study of Direct F. Scarlet, Egyptian Journal of Aquatic Res., 31(1): 1110-0354.
19. Qadeer, R., 2004. Adsorption of ruthenium ions on activated charcoal: influence of temperature on the kinetics of the adsorption process, Journal of Zhejiang University Science, 6B(5): 353-356.
20. Nwabanne, J.T. and P.K. Igbokwe, 2008. kinetics and equilibrium modeling of Nickel adsorption by cassava peel, Journal of Engineering and Applied Sciences, 3(11): 829-834.
21. Sekar, M., V. Sakthi and S. Rengaraj, 2004. Kinetics' and equilibrium studies of lead (11) onto activated carbon prepared from coconut shell, Journal of Colloid and Interface Science, 279: 307-313.
22. Lagergren, S. and B.K. Svenska, 1998. Zur theorie der sogenannten adsorption geloester stoffe, Veternskapsakad Handlingar, 24(4): 1-39.
23. Qadeer, R. and J. Hanif, 1994. Kinetics of zirconium ions adsorption on activated charcoal from aqueous solution, American journal of Biochemistry and Biotechnology, 3(2): 34-43.
24. Asghari, F., M. Jahanshahi and A.A. Ghoreyshi, 2012. A Comparative Study of Agarose-Nickel Prototype Composite Adsorbent and Commercial Streamline Deae Adsorbent: Physical and Hydrodynamical Assessments, Iranica Journal of Energy and Environment, 3(4): 291-298.
25. Gaikwad, R.W., 2012. Removal of Lead by Reverse Fluidization Using Granular Activated Carbon, Iranica Journal of Energy and Environment, 3(4): 314-319.
26. Koel, B., S.T. Ramesh, R. Gandhimathi, P.V. Nidheesh and K.S. Bharathi, 2012. A Novel Agricultural Waste Adsorbent, Watermelon Shell for the Removal of Copper from Aqueous Solutions, Iranica Journal of Energy and Environment, 3(2): 143-156.
27. Saberi, A., 2012. Comparison of Pb^{2+} Removal Efficiency by Zero Valent Iron Nanoparticles and Ni/Fe Bimetallic Nanoparticles, Iranica Journal of Energy and Environment, 3(2): 189-196.
28. Gandhimathi, R., S.T. Ramesh, V. Sindhu and P.V. Nidheesh, 2012. Single and Tertiary System Dye Removal from Aqueous Solution Using Bottom Ash: Kinetic and Isotherm Studies, Iranica Journal of Energy and Environment, 3(1): 35-45.
29. Ghorbani, G., H. Eisazadeh and A.A. Ghoreyshi, 2012. Removal of Zinc Ions from Aqueous Solution Using Polyaniline Nanocomposite Coated on Rice Husk, Iranica Journal of Energy & Environment, 3(1): 66-71.
30. Bharathi, K.S. and S.P. Ramesh, 2012. Equilibrium, Thermodynamic and Kinetic Studies on Adsorption of a Basic Dye by Citrullus Lanatus Rind, Iranica Journal of Energy and Environment, 3(1): 23-34.
31. Radneia H., A.A. Ghoreyshi and H. Younesi, 2011. Isotherm and Kinetics of Fe(II) onto Chitosan in a Batch Process, Iranica Journal of Energy and Environment, 2(3): 250-257.

Persian Abstract

DOI: 10.5829/idosi.ijee.2013.04.04.08

چکیده

کربن فعال از پوست کاساوا تهیه گردید و خصوصیات الکتروشیمیایی آن از قبیل مقدار رطوبت، مواد فرار و مساحت سطح مشخص گردید. اثرات پارامترهای مختلف مانند میزان جاذب، زمان تماس، دمای جذب و pH در جهت بهینه سازی شرایط برای حداکثر جذب بررسی گردید. مکانیزم سرعت جذب با استفاده از معادلات لاگرگرن شبه درجه اول و معادله سوانته آرنیوس بررسی گردید و معادله انرژی آزاد گیبس برای تعیین ترمودینامیک جذب به کار گرفته شد. ایزوترمهای جذب توسط معادله ایزوترم فرندلیچ و لانگمیر و همچنین ایزوترم تمکین که اثرات برهمکنش های غیر مستقیم جاذب و جذب شونده را ارائه می کند، مورد بررسی قرار گرفت. میزان برازش داده ها با استفاده از ضریب همبستگی (R^2) تعیین شد. ثابت ترمودینامیکی ($\mathbf{K_{ad}}$)، انرژی آزاد استاندارد ($\Delta\mathbf{G^0}$)، آنتالپی ($\Delta\mathbf{H^0}$) و آنتروپی ($\Delta\mathbf{S^0}$) برای پیش بینی ماهیت جذب محاسبه گردید. نتایج به دست آمده کارامدی کربن فعال حاصل از پوست کاساوا را بعنوان جاذبی مناسب برای تصفیه پساب نشان می‌دهد.